Cluster model for the ionic product of water: Accuracy and limitations of common density functional methods

Daniel Svozil and Pavel Jungwirth*

Institute of Organic Chemistry and Biochemistry,

Academy of Sciences of the Czech Republic

Flemingovo nám. 2, 166 10, Prague 6, Czech Republic

* e-mail: pavel.jungwirth@uochb.cas.cz

In the present study, the performance of six popular density functionals (B3LYP, PBE0, BLYP, BP86, PBE, SVWN) for the description of the autoionization process in the water octamer was studied. As a benchmark, MP2 energies with complete basis sets limit extrapolation and CCSD(T) correction were used. At this level the autoionized structure lies 28.5 kcal.mol^{-1} above the neutral water octamer. Accounting for zero point energy lowers this value by 3.0 kcal.mol^{-1}. The transition state of the proton transfer reaction, lying only 0.7 kcal.mol^{-1} above the energy of the ionized system,

was identified at the MP2/aug-cc-pVDZ level of theory. Different density functionals describe the reactant and product with varying accuracy, while they all fail to characterize the transition state. We find improved results with hybrid functionals compared to the gradient-corrected ones. In particular, B3LYP describes the reaction energetics within 2.5 kcal.mol^{-1} of the benchmark value. Therefore, this functional is suggested to be preferably used both for Car-Parinello molecular dynamics and QM/MM simulations of autoionization of water.

1 Introduction

The finite value of pH of neat water is due to its remarkable ability to spontaneously autoionize in a strongly endothermic process. Water molecules transiently ionize due to electric field fluctuations. The nascent ions normally recombine within a few femtoseconds, but rarely (about once every eleven hours per molecule at 25^{o}C) the local hydrogen bonding rearranges before the geminate recombination, and the pair of ions (formally H^+ and OH^-) hydrate independently continuing their separate existence for about 70 ms.[1] The tendency for autoionization is proportional to the strength of hydration of these ions. The kinetics and energetics of the autoionization reaction depends upon the thermodynamic conditions, such as temperature, density, or pressure.[2–6] It has also been shown that the hydration mechanism of ions and pH change dramatically and non-monotically upon reaching the

supercritical region.[6,7]

In water, the H^+ and OH^- ions of course do no exist as isolated species, but they form strong bonds with surrounding water molecules. The picture of hydrated H^+ was refined by Eigen,[8–10] as well as Zundel and Metzger[11] who advocated the presence of larger complexes such as $H_9O_4^+$ and $H_5O_2^+$, respectively. In the former "Eigen cation" the central hydronium ion (H_3O^+) is strongly hydrogen bonded to three water molecules, while in the later "Zundel cation" proton lies midway between two water molecules. Bulk investigations of the detailed structure of these transient complexes are experimentally difficult, therefore, many experimental,[12–17] as well as theoretical[18–24] studies have been devoted to the molecular description of the hydrated proton in water clusters. Zundel motif was identified by theoretical analysis of infrared spectra of clusters with H^+ and $6-8$ water molecules, while an embedded Eigen core was found in clusters with more than 8 waters.[25] As far as hydration of OH^- is concerned, theory[26–28] and experiments[29–31] converged to unified view only recently. The present picture is that the first solvation shell of OH^- is comprised of three strongly hydrogen-bonded water molecules.

Related to the structural aspects is the mechanism of the anomalously high mobility of the proton in water, which is approximately five times higher than the mobility of ions of a size similar to H_3O^+.[32] The classical attempt to explain this observation is via the famous Grotthuss mechanism.[33,34] Based on ab initio molecular dynamics it was suggested[35] that the hydrated proton forms a moving defect in the hydrogen bonded network with "Eigen" and

"Zundel" structures representing limiting cases. Such proton transfer does not match with the traditional view, since the interconversion of the hydrated proton is not limited by the proton motion itself, but rather by rearrangements of water molecules leading to rates considerably larger than those of conventional diffusion. The Car-Parinello (CPMD) calculations show that this "structural diffusion" is driven by fluctuations in the second solvation shell of H_3O^+.[35] Recently, using CPMD combined with transition path sampling,[36–38] it was shown[1] that the transfer of a proton in the O-H...O system represents a first step, and that the dissociation of O-H bonds is driven by the concerted changes in the electric field and in the hydrogen bond network. Despite extensive studies employing different theoretical approaches,[26,35,39–43] the detailed mechanism of proton transfer is still debated.

Similarly to hydronium, OH^- also exhibits anomalously high mobility in water. It was generally believed that the motion of OH^- in water resembles that of proton[44] because the hydroxide ion can be viewed as a "proton hole" (i.e., a water molecule with a missing proton).[45] This picture was later challenged by ab initio CPMD studies.[46,47] The first study[46] suggested that transport occurs when an approximately square-planar configuration $OH(H_2O)_4^-$ converts to an $OH(H_2O)_3^-$ system. Based on a later CPMD study,[47] a more complex four step mechanism for hydroxide transport was proposed. A somewhat different mechanism was observed in another CPMD study of concentrated NaOH and KOH solutions.[48]

The eludication of the structural and dynamical aspects of the water

autoionization process continues to be an extremely challenging problem. Carr-Parinello molecular dynamics simulation methods, based on density functional theory (DFT), employing primarily the BLYP functional, have played a pivotal role in the theoretical description. Clearly, the success of such simulations depends to a large extent on the quality of the employed DFT method. In the present study, we evaluated the performance of six popular density functionals, covering local density approximation, gradient-corrected, and hybrid density functionals, for describing the water autoionization process. As a model system we have chosen a finite size water cluster, for which we are able to perform benchmark ab initio calculations consisting of complete basis set limit MP2 calculations with a CCSD(T) correction. In particular, we employed the cubic water octamer, that was shown to exist in two nearly isoenergetic forms having very similar structures of D_{2d} and S_4 symmetries.[49–51] The cubic water octamer (in S_4 symmetry) was used in our study since it represents, in its ionized form, a natural merge of hydrated H_3O^+ in its Eigen form (i.e. $H_3O^+(H_2O)_3$) and hydrated OH^- (i.e. $OH^-(H_2O)_3$). Moreover, water octamer is the smallest cluster which we found to support a H_3O^+/OH^- ion pair as a minimum on the potential energy surface.

2 Methods

A set of DFT methods including local density approximation LDA (SVWN), gradient-corrected GGA (BLYP, BP86, PBE), and hybrid density functionals (B3LYP, PBE0) with two different basis sets (6-31+G* and aug-cc-pVDZ) was used (see Table 1) to characterize the autoionization process in cubic water octamer (denoted as 8W), i.e., proton transfer from hydrated hydronium to hydrated hydroxide ions (the ionic structure being further denoted as 6W) (see Figure 1). The results were compared to high-level ab initio calculations consisting of MP2 energies evaluated at the complete basis set limit (CBS), refined by the CCSD(T) correction.

Complete basis set (CBS) MP2 energies were estimated using an extrapolation scheme[52,53] utilizing Dunning's augmented correlation consistent basis sets of double and triple zeta quality:[54]

$$E^{\mathrm{HF}}_{\mathrm{CBS}} = E^{\mathrm{HF}}_{\mathrm{aug-cc-pVDZ}} + \left(E^{\mathrm{HF}}_{\mathrm{aug-cc-pVTZ}} - E^{\mathrm{HF}}_{\mathrm{aug-cc-pVDZ}}\right)/0.760691 \quad (1)$$

$$E^{\mathrm{MP2}}_{\mathrm{CBS}} = E^{\mathrm{MP2}}_{\mathrm{aug-cc-pVDZ}} + \left(E^{\mathrm{MP2}}_{\mathrm{aug-cc-pVTZ}} - E^{\mathrm{MP2}}_{\mathrm{aug-cc-pVDZ}}\right)/0.703704 \quad (2)$$

Due to the relatively high computational demands of MP2 calculations with the employed basis sets, the approximate resolution of identity MP2 (RI-MP2) method[55,56] was used for geometry optimizations. In the RI-MP2 approximation two-electron four-centers integrals are replaced by linear combinations of two-electron three-centers integrals, via the introduction of an auxiliary fitting basis set.[55–57] This results in a speedup of RI-MP2 cal-

culations compared with standard MP2 that depends on the details of the calculations, easily reaching an order of magnitude.[55,57,58] Regarding the accuracy, it has been shown on several systems that with an accurate choice of the auxiliary fitting basis energies and structures computed with MP2 and RI-MP2 methods do not show significant differences.[55,58,59]

Assuming that the difference between CCSD(T) and MP2 energies exhibits only a small basis set dependence,[60,61] CCSD(T) energies at complete basis set level can be estimated as:

$$E_{\mathrm{CBS}}^{\mathrm{CCSD(T)}} = E_{\mathrm{CBS}}^{\mathrm{MP2}} + \left(E_{\mathrm{aug-cc-pVDZ}}^{\mathrm{CCSD(T)}} - E_{\mathrm{aug-cc-pVDZ}}^{\mathrm{MP2}} \right) \tag{3}$$

where $E_{\mathrm{aug-cc-pVDZ}}^{\mathrm{CCSD(T)}}$ and $E_{\mathrm{aug-cc-pVDZ}}^{\mathrm{MP2}}$ are computed at MP2/aug-cc-pVTZ geometries. Zero-point vibrational energies calculated at the MP2/aug-cc-pVDZ level were also added to $E_{\mathrm{CBS}}^{\mathrm{CCSD(T)}}$ energies, yielding thus relative enthalpies. Stationary points were verified to be minima via standard frequency calculations (positive Hessian eigenvalues for all vibrational modes), that were also used to calculate zero-point and thermal contributions to Gibbs free energy at 298.15 K and 1 atm.

In order to investigate the barrier height between the two minimum conformations (neutral 8W and autoionized 6W), a saddle point was localized by means of the MP2/aug-cc-pVDZ transition state optimization. Thermodynamic functions were taken from partition functions computed from MP2/aug-cc-pVDZ characteristics (ignoring the one imaginary frequency at

saddle point) according to a rigid rotor/harmonic oscillator/ideal gas approximation.

RI-MP2 optimizations were carried out with the computer code Turbomole 4.7,[62] CCSD(T) calculations were performed using Molpro 2002.6[63] package, while the remaining calculations were done with Gaussian 03.[64]

3 Results

It is worth to start by mentioning that in the gas phase the set of $H_3O\bullet$ and $\bullet OH$ radicals is more stable than the corresponding ion pair. However, in the present system containing six additional water molecules the ions lie energetically well below the radical pair, as in liquid water. Three water molecules represent the tight first solvation shell of both H_3O^+ and OH^-.[19,28,31] When these two solvation shell are brought close each to other, $H_3O^+(H_2O)_3$ and $OH^-(H_2O)_3$ form a cluster with a cubic structure, where the two ions lie in the opposite corners (the 6W structure). This structure resembles in oxygen positions the neutral water octamer in S_4 symmetry (the 8W structure)[65] (see Figure 1).

3.1 Geometry

The D_{2d} and S_4 structures of water octamer each contain 12 H-bonds: four in each of two cyclic tetramer subunits, and four bridging the two tetramers. The two structures are distinct in having the H-bonds within the two tetramers

oriented in the opposite (D_{2d}) or same (S_4) directions. In our study, the S_4 structure was employed. The results for the RI-MP2/aug-cc-pVTZ geometry of the water octamer (8W) show that the calculated optimal O-H distance of dangling bonds (0.96126 Å) is by $0.01 - 0.03$ Å shorter than that of the hydrogen bonded O-H. The H-O-H angle of water molecules with dangling hydrogens ($\sim 106.41^o$) is by $\sim 2.5^o$ larger than that in hydrogen-bonded waters $\sim 103.95^o$. The autoionized 6W structure is less symmetric than 8W structure, but the characteristics cubic-like shape is nevertheless retained (see Figure 1). The optimal O-H distance in hydronium ion H_3O^+ is slightly longer (~ 1.03 Å), while that in OH^- is very close to that in neutral water.

The geometries of 8W and 6W minimal structures calculated using different DFT functionals were compared to the geometry obtained with the RI-MP2 method utilizing the aug-cc-pVTZ basis set. For this comparison, root-mean-square deviations (RMSD) between DFT and RI-MP2/aug-cc-pVTZ minima were evaluated (see Table 2). Generally, while the geometry of the neutral water octamer is reproduced reasonably well by all employed functionals, the description of the autoionized structure turns out to be more difficult. As an extreme case, the local density approximation represented by the SVWN functional completely fails to describe the ionic product. Instead of hydronium and oxonium ions surrounded by six water molecules, SVWN predicts a conformation with three oxonium and three hydronium ions as the lowest energy structure. In addition, the SVWN geometry of 8W is of the lowest accuracy among all studied functionals. LDA, which is

known for its drastic overbinding of various water clusters,[66] and, generally, for its moderate accuracy, clearly cannot be used for any quantitative water simulation.

The employed gradient-corrected functionals (BLYP, BP86, PBE) describe the 8W structure with still reasonable accuracy (RMSD of $\sim 0.04-0.06$ Å), which is only marginally worse than that of the hybrid functionals. The RMSD values for autoionized 6W system are, however, somewhat larger (RMSD of $\sim$ 0.1 Å) for GGA functionals. In terms of both neutral and ionic clusters geometries, the most accurate DFT results are obtained using both hybrid functionals - B3LYP and PBE0 (see Table 2). These structures are very close to the MP2/aug-cc-pVTZ benchmark (RMSD $\sim$ 0.03 Å).

As mentioned above, the correct description of the geometry of ionic system is more problematic than that of the water molecular cluster. In our DFT calculations, apart from structures that are close to benchmarking structures (RMSD up to 0.11 Å), we obtained in two cases also distorted geometries with RMSD values of 0.6 - 0.7 Å. In these structures, the oxygen-oxygen distances between the ionic species and the first solvation shell water molecules are retained, but the hydronium cation with its three tightly bound water molecules is rotated with respect to hydrated hydroxide anion, so that the cluster structure is not cubic-like anymore. This somewhat strange distortion, which is not accompanied by any charge neutralization, occurs only for B3LYP and BLYP functionals utilizing the aug-cc-pVDZ basis set.

3.2 Energy

Benchmark calculations were performed both for the neutral water octamer 8W and for the corresponding autoionized 6W cluster. The resulting energy differences between these two structures, showing the importance of including higher order electron correlation corrections and basis set extrapolation, are summarized in Tables 3 and 4. Our best estimate of potential energy difference between 8W and 6W structures is $\Delta E_{8W-6W} = -28.51$ kcal.mol^{-1}, and that of the enthalpy difference equals to $\Delta H_{8W-6W} = -25.10$ kcal.mol^{-1}. As the primary interest of our work is the benchmarking of DFT methods for energy calculations, the value of $\Delta E_{8W-6W} = -28.51$ kcal.mol^{-1} is used for further comparison.

The free energy difference between 8W and 6W structures $\Delta G_{8W-6W} = -24.25$ kcal.mol^{-1} obtained from the above enthalpy difference by including a harmonic oscillator/free rotor/ideal gas entropy term at 298.15 K, can be compared to the bulk water value $\Delta G = -RT \ln K = -19.1$ kcal.mol^{-1}, corresponding to pH = 7. The correspondence between these two values is reasonable, taking into account, that the later value is pertinent to bulk water, from which our cluster systems differ significantly. In order to mimic the bulk environment we employed the COSMO implicit solvent model[67] together with RI-MP2/aug-cc-pVDZ calculations for the 8W and 6W structures. Upon COSMO solvation, the difference in energy between 8W and 6W structures drops by 3.4 kcal.mol^{-1}. Adding this difference to the above ΔG_{8W-6W} yields a value of -20.85 kcal.mol^{-1}, which is rather close to the

bulk water value of -19.1 kcal.mol^{-1}. This fact further justifies the choice of the present benchmark system.

The MP2/aug-cc-pVDZ investigation of the transition between the 8W and 6W clusters reveals, that there exists a simple reaction coordinate - the distance between hydrogen and oxygen in hydronium cation, the change of which triggers a proton transfer over two water molecules (see Figure 2). The MP2/aug-cc-pVDZ transition state lies 27.4 kcal.mol^{-1} above the 8W state, and only 0.7 kcal.mol^{-1} above 6W structure on the potential energy surface (see Table 4 and Figure 3). This very low barrier, which disappears upon inclusion of the zero point energy correction, indicates that in the experiment the autoionized 6W structure would on a short time scale spontaneously interconvert into the neutral water octamer. Nevertheless, the 6W geometry is a well defined minimum at the potential energy surface and we can, therefore, use the energy difference between the 8W and 6W structures for benchmarking purposes.

The influence of the basis set on the energy differences was investigated using the MP2 method with three different basis sets: Pople's 6-31+G* basis set and Dunning's correlation consistent aug-cc-pVDZ and aug-cc-pVTZ basis sets (see Table 4). Note that $|\Delta\ E_{8W-6W}|$ decreases slightly with increasing basis set quality, with Dunning's basis set of triple-ζ quality being very close (by 0.3 kcal.mol^{-1}) to the complete basis set limit (see Table 3). The barrier height also marginally decreases upon moving from the 6-31+G* to the aug-cc-pVDZ basis set.

We have then performed a series of DFT calculations extracting the relative energies of the 8W and 6W clusters (Table 5). Only the Δ E_{8W-6W} values were calculated in our study, since the low-lying transition state could not be located using any of the used DFT functionals, which are in general known to underestimate reaction barriers.[68–70] For Δ E_{8W-6W} we find improved results from two tested hybrid functionals (B3LYP and PBE0) compared to those from non-hybrid gradient-corrected functionals (BLYP, BP86, and PBE). The decrease of $|\Delta$ $E_{8W-6W}|$ with increasing quality of basis set is also observed for DFT methods. The deficiencies following from the approximate density functional largely cancel out with finite basis size, bringing results with the smaller 6-31+G* basis set closer to the benchmark value of $\Delta E^{CBS}_{8W-6W} = -28.51$ kcal.mol^{-1}, with the B3LYP/6-31+G* value of -25.84 kcal.mol^{-1} being the closest. The second hybrid functional, PBE0, also gives a reasonable result of -24.24 kcal.mol^{-1}. All gradient corrected functionals have errors higher than hybrid ones, falling within the ~ 6 kcal.mol^{-1} range for BLYP, and ~ 10 kcal.mol^{-1} for BP86 and PBE.

4 Discussion and Conclusions

We have investigated and benchmarked the performance of common DFT methods, including local density approximation, gradient-corrected and hybrid functionals, for the description of autoionization of water. To this end, we have compared the structural and energetic properties of cubic water oc-

tamer to the corresponding cluster consisting of a hydronium cation with three tightly hydrogen-bonded water molecules and a hydroxide anion also with three first solvation water molecules. Our study focuses on the static picture, since it has been demonstrated recently, that the overall accuracy of the hybrid functionals deduced from static calculations transfers to the dynamical properties.[66]

The geometries obtained by the above DFT functionals were compared to accurate results from a MP2/aug-cc-pVTZ optimization. The DFT energies were benchmarked against complete basis set limit extrapolated MP2 values with a CCSD(T) correction. While the geometry of the cubic neutral water octamer is described reasonably well with all functionals employed, the autoionized system represents a bigger challenge for DFT methods, LDA approximation failing completely in its description. The energy difference between these two structures ΔE_{8W-6W} for the B3LYP (PBE0) hybrid functional is about 2.5 (4.0) kcal.mol^{-1} smaller in absolute value than that of the benchmark ab initio calculations. All gradient-corrected functionals overestimate the stability of the ionic structure more than the hybrid functionals (e.g. BLYP gives ΔE_{8W-6W} smaller by 6.3 kcal.mol^{-1} compared to the benchmark value, the other gradient-corrected functionals performing even worse). Because of the higher relative stability of the autoionized structure predicted by DFT methods (see Figure 3), the ionic forms will be overpopulated in DFT-based dynamics. None of the density functionals employed was successful in localizing the transition state between the two structures. This

is not surprising, as the MP2/aug-cc-pVDZ transition state lies in energy only 0.7 kcal.mol^{-1} above the 6W cluster, and DFT methods consistently underpredict barrier heights.[68–70]

Our benchmarking indicates that only moderate accuracy can be expected from BLYP or other gradient-corrected functionals. Much better results are obtained with hybrid functionals (B3LYP, PBE0). We employed the functionals with Gaussian basis sets, but similar performance can also be expected with plane wave expansion.

Dynamical calculations with hybrid functionals are becoming feasible, since efficient calculations of Hartree-Fock exchange within a plane wave framework have been achieved already.[71–73] Another approach, applicable to liquid water molecular dynamics simulations,[74] is the use of a mixed quantum mechanics/molecular mechanics (QM/MM) technique. Within this approach, the most important region containing the particles under investigations (i.e., both H_3O^+ and OH^- with their tight solvation shells) should be described either by the B3LYP functional, or, if computationally feasible, by the RI-MP2 method, while the rest of the aqueous system is treated using an empirical force field.

Acknowledgement

This work was supported by the Czech Ministry of Education (grant LC512) and by the research project Z4 055 905. P. J. acknowledges support from the

Granting Agency of the Czech Republic (grant 202/06/0286).

References

1. Geissler, P.; Dellago, C.; Chandler, D.; Hutter, J.; Parrinello, M. *Science* **2001,** *291,* 2121 – 2124.

2. Eisenberg, D.; Kauzmann, W. *The Structure and Properties of Water;* Oxford University Press: Oxford, UK, 1969.

3. Franks, F. *Water: A matrix of life.;* Royal Society of Chemistry: Cambridge, UH, 2000.

4. Ball, P. *Life's Matrix: A Biography of Water.;* University of California Press: Berkeley, USA, 2001.

5. Ohtaki, H. *Journal of Molecular Liquids* **2003,** *103,* 3 – 13.

6. Yagasaki, T.; Iwahashi, K.; Saito, S.; Ohmine, I. *Journal of Chemical Physics* **2005,** *122,*.

7. Mesmer, R.; Marshall, W.; Palmer, D.; Simonson, J.; Holmes, H. *Journal of Solution Chemistry* **1988,** *17,* 699 – 718.

8. Wicke, E.; Eigen, M.; Ackermann; *Zeitschrift Fur Physikalische Chemie* **1954,** *1,* 340 – 364.

9. Eigen, M. *Angewandte Chemie* **1963,** *75,* 489.

10. Eigen, M. *Angewandte Chemie International Edition* **1964,** *3,* 1.

11. Zundel, G.; Metzger, H. *Zeitschrift Fur Physikalische Chemie* **1968,** *58,* 225 – 245.

12. Begemann, M.; Gudeman, C.; Pfaff, J.; Saykally, R. *Physical Review Letters* **1983,** *51,* 554 – 557.

13. Jiang, J.; Wang, Y.; Chang, H.; Lin, S.; Lee, Y.; Niedner-Schatteburg, G.; Chang, H. *Journal of the American Chemical Society* **2000,** *122,* 1398 – 1410.

14. Kim, J.; Schmitt, U.; Gruetzmacher, J.; Voth, G.; Scherer, N. *Journal of Chemical Physics* **2002,** *116,* 737 – 746.

15. Asmis, K.; Pivonka, N.; Santambrogio, G.; Brummer, M.; Kaposta, C.; Neumark, D.; Woste, L. *Science* **2003,** *299,* 1375 – 1377.

16. Miyazaki, M.; Fujii, A.; Ebata, T.; Mikami, N. *Science* **2004,** *304,* 1134 – 1137.

17. Shin, J.; Hammer, N.; Diken, E.; Johnson, M.; Walters, R.; Jaeger, T.; Duncan, M.; Christie, R.; Jordan, K. *Science* **2004,** *304,* 1137 – 1140.

18. Xie, Y.; Remington, R.; Schaefer, H. *Journal of Chemical Physics* **1994,** *101,* 4878 – 4884.

19. Wei, D.; Salahub, D. *Journal of Chemical Physics* **1994,** *101,* 7633 – 7642.

20. Ciobanu, C.; Ojamae, L.; Shavitt, I.; Singer, S. *Journal of Chemical Physics* **2000,** *113,* 5321 – 5330.

21. Sobolewski, A.; Domcke, W. *Journal of Physical Chemistry A* **2002,** *106,* 4158 – 4167.

22. Pickard, F.; Pokon, E.; Liptak, M.; Shields, G. *Journal of Chemical Physics* **2005,** *122,*.

23. McCoy, A.; Huang, X.; Carter, S.; Landeweer, M.; Bowman, J. *Journal of Chemical Physics* **2005,** *122,* 061101.

24. Huang, X.; Braams, B.; Bowman, J. *Journal of Chemical Physics* **2005,** *122,* 044308.

25. Headrick, J.; Diken, E.; Walters, R.; Hammer, N.; Christie, R.; Cui, J.; Myshakin, E.; Duncan, M.; Johnson, M.; Jordan, K. *Science* **2005,** *308,* 1765 – 1769.

26. Tuckerman, M.; Marx, D.; Klein, M.; Parrinello, M. *Science* **1997,** *275,* 817 – 820.

27. Chen, B.; Park, J.; Ivanov, I.; Tabacchi, G.; Klein, M.; Parrinello, M. *Journal of the American Chemical Society* **2002,** *124,* 8534 – 8535.

28. Asthagiri, D.; Pratt, L.; Kress, J.; Gomez, M. *Chemical Physics Letters* **2003,** *380,* 530 – 535.

29. Robertson, W.; Diken, E.; Price, E.; Shin, J.; Johnson, M. *Science* **2003,** *299,* 1367 – 1372.

30. Botti, A.; Bruni, F.; Imberti, S.; Ricci, M.; Soper, A. *Journal of Chemical Physics* **2003,** *119,* 5001 – 5004.

31. Asthagiri, D.; Pratt, L.; Kress, J.; Gomez, M. *PNAS* **2004,** *101,* 7229 – 7233.

32. Robinson, R. A.; Stokes, R. H. *Electrolyte Solutions;* Butterworths: London, UK, 1959.

33. de Grotthuss, C. J. T. *Annales de Chimie* **1806,** *58,* 54 – 73.

34. Agmon, N. *Chemical Physics Letters* **1995,** *244,* 456 – 462.

35. Marx, D.; Tuckerman, M.; Hutter, J.; Parrinello, M. *Nature* **1999,** *397,* 601 – 604.

36. Dellago, C.; Bolhuis, P.; Csajka, F.; Chandler, D. *Journal of Chemical Physics* **1998,** *108,* 1964 – 1977.

37. Dellago, C.; Bolhuis, P.; Geissler, P. *Advances In Chemical Physics, Vol 123* **2002,** *123,* 1 – 78.

38. Bolhuis, P.; Chandler, D.; Dellago, C.; Geissler, P. *Annual Review of Physical Chemistry* **2002,** *53,* 291 – 318.

39. Ojamae, L.; Shavitt, I.; Singer, S. *Journal of Chemical Physics* **1998,** *109,* 5547 – 5564.

40. Schmitt, U.; Voth, G. *Journal of Chemical Physics* **1999,** *111,* 9361 – 9381.

41. Marx, D.; Tuckerman, M.; Parrinello, M. *Journal of Physics - Condensed Matter* **2000,** *12,* A153 – A159.

42. Walbran, S.; Kornyshev, A. *Journal of Chemical Physics* **2001,** *114,* 10039 – 10048.

43. Asthagiri, D.; Pratt, L.; Kress, J. *PNAS* **2005,** *102,* 6704 – 6708.

44. Agmon, N. *Chemical Physics Letters* **2000,** *319,* 247 – 252.

45. Huckel, E. Z. *Z. Elektrochem. Angew. Phys. Chem.* **1928,** *34,* 546.

46. Tuckerman, M.; Laasonen, K.; Sprik, M.; Parrinello, M. *Journal of Chemical Physics* **1995,** *103,* 150 – 161.

47. Tuckerman, M.; Marx, D.; Parrinello, M. *Nature* **2002,** *417,* 925 – 929.

48. Chen, B.; Ivanov, I.; Park, J.; Parrinello, M.; Klein, M. *Journal of Physical Chemistry B* **2002,** *106,* 12006 – 12016.

49. Tsai, C.; Jordan, K. *Journal of Chemical Physics* **1991,** *95,* 3850 – 3853.

50. Tsai, C.; Jordan, K. *Journal of Physical Chemistry* **1993,** *97,* 5208 – 5210.

51. Fanourgakis, G.; Apra, E.; Xantheas, S. *Journal of Chemical Physics* **2004,** *121,* 2655 – 2663.

52. Helgaker, T.; Klopper, W.; Koch, H.; Noga, J. *Journal of Chemical Physics* **1997,** *106,* 9639 – 9646.

53. Halkier, A.; Helgaker, T.; Jorgensen, P.; Klopper, W.; Olsen, J. *Chemical Physics Letters* **1999,** *302,* 437 – 446.

54. Kendall, R.; Dunning, T.; Harrison, R. *Journal of Chemical Physics* **1992,** *96,* 6796 – 6806.

55. Feyereisen, M.; Fitzgerald, G.; Komornicki, A. *Chemical Physics Letters* **1993,** *208,* 359 – 363.

56. Vahtras, O.; Almlof, J.; Feyereisen, M. *Chemical Physics Letters* **1993,** *213,* 514 – 518.

57. Jurecka, P.; Nachtigall, P.; Hobza, P. *Physical Chemistry Chemical Physics* **2001,** *3,* 4578 – 4582.

58. Bernholdt, D.; Harrison, R. *Chemical Physics Letters* **1996,** *250,* 477 – 484.

59. Feller, D.; Apra, E.; Nichols, J.; Bernholdt, D. *Journal of Chemical Physics* **1996,** *105,* 1940 – 1950.

60. Koch, H.; Fernandez, B.; Christiansen, O. *Journal of Chemical Physics* **1998,** *108,* 2784 – 2790.

61. Jurecka, P.; Hobza, P. *Chemical Physics Letters* **2002,** *365,* 89 – 94.

62. Ahlrichs, R.; Bar, M.; Haser, M.; Horn, H.; Kolmel, C. *Chemical Physics Letters* **1989,** *162,* 165.

63. Werner, H.-J. *et al.* "MOLPRO, version 2002.6, a package of ab initio programs", 2003 see http://www.molpro.net.

64. Frisch, M. J. *et al. Gaussian 03;* Gaussian, Inc.: Pittsburgh PA, U.S.A., 2003.

65. Xantheas, S.; Apra, E. *Journal of Chemical Physics* **2004,** *120,* 823 – 828.

66. Todorova, T.; Seitsonen, A. P.; Hutter, J.; Kuo, I. W.; Mundy, C. J. *Journal of Physical Chemistry B* **2006,** *110,* 3685 – 3691.

67. Klamt, A.; Schuurmann, G. *Journal of The Chemical Society - Perkin Transactions 2* **1993,** 799 – 805.

68. Andzelm, J.; Baker, J.; Scheiner, A.; Wrinn, M. *International Journal of Quantum Chemistry* **1995,** *56,* 733 – 746.

69. Durant, J. *Chemical Physics Letters* **1996,** *256,* 595 – 602.

70. Koch, W.; C., H. M. *A Chemist's Guide to Density Functional Theory.;* Wiley-VCH: Weinheim, Federal Republic of Germany, 2000.

71. Gygi, F.; Baldereschi, A. *Physical Review B* **1986,** *34,* 4405 – 4408.

72. Chawla, S.; Voth, G. *Journal of Chemical Physics* **1998,** *108,* 4697 – 4700.

73. Paier, J.; Hirschl, R.; Marsman, M.; Kresse, G. *Journal of Chemical Physics* **2005,** *122,*.

74. Xenides, D.; Randolf, B.; Rode, B. *Journal of Chemical Physics* **2005,** *122,*.

75. Dirac, P. A. M. *Proceedings of the Royal Sciety (London) A* **1929,** *123,* 714.

76. Slater, J. C. *Physical Review* **1951,** *81,* 385 – 390.

77. Becke, A. *Physical Review A* **1988,** *38,* 3098 – 3100.

78. Perdew, J.; Burke, K.; Ernzerhof, M. *Physical Review Letters* **1996,** *77,* 3865 – 3868.

79. Vosko, S.; Wilk, L.; Nussair, M. *Canadian Journal of Physics* **1980,** *58,* 1200.

80. Perdew, J. *Physical Review B* **1986,** *33,* 8822 – 8824.

81. Lee, C.; Yang, W.; Parr, R. *Physical Review B* **1988,** *37,* 785 – 789.

82. Perdew, J.; Wang, Y. *Physical Review B* **1992,** *45,* 13244 – 13249.

Table 1: Definitions of exchange-correlation functionals used in this study. The exchange and correlation functionals are described in the following references: Slater-Dirac S,[75,76] Becke B88,[77] Perdew-Burke-Ernzerhof PBE,[78] Vosko-Wilk-Nussair VWN,[79] Perdew P86,[80] Lee-Yang-Parr LYP,[81] Perdew-Wang PW.[82]

Functional	Type	Exchange	Correlation
B3LYP	HYB	0.8S + 0.72B88 + 0.2HF	0.19VWN(III)+0.81LYP
PBE0	HYB	0.75(S + PBE(X)) + 0.25HF	PW + PBE(C)
BLYP	GGA	S + B88	LYP
BP86	GGA	S + B88	VWN(V) + P86
PBE	GGA	S + PBE(X)	PW + PBE(C)
SVWN	LDA	S	VWN

Table 2: Differences in geometries (in Å) obtained by all tested functionals for both neutral and ionic systems, respectively, given as RMSD with respect to benchmark MP2/aug-cc-pVTZ geometry. Note, that the aug-cc-pVDZ energies of B3LYP and BLYP functionals were evaluated for the twisted minimal geometries (see part 3.1 for details).

Method	Basis set	6W	8W
MP2	aug-cc-pVTZ	0.0	0.0
B3LYP	6-31+G*	0.033	0.033
	aug-cc-pVDZ	0.656	0.027
PBE0	6-31+G*	0.069	0.043
	aug-cc-pVDZ	0.021	0.029
BLYP	6-31+G*	0.100	0.049
	aug-cc-pVDZ	0.652	0.044
BP86	6-31+G*	0.107	0.063
	aug-cc-pVDZ	0.037	0.058
PBE	6-31+G*	0.096	0.055
	aug-cc-pVDZ	0.028	0.048
SVWN	6-31+G*	-	0.200
	aug-cc-pVDZ	-	0.220

Table 3: Complete basis et limit potential energy, and enthalpy differences between 8W, and 6W systems. The last row of the table corresponds to ΔH evaluated at 298.15 K and 1 atm. The MP2 complete basis set limit was obtained by extrapolating aug-cc-pVDZ and aug-cc-pVTZ energies calculated at the aug-cc-pVTZ geometry, CCSD(T) correction was calculated with aug-cc-pVDZ basis set at the MP2/aug-cc-pVTZ geometry, and ZPVE contribution was obtained at the MP2/aug-cc-pVDZ//MP2/aug-cc-pVDZ level of theory.

Method	Δ E_{8W-6W} [kcal.mol^{-1}]
MP2 CBS	-25.29
MP2 CBS + Δ CCSD(T)	-28.51
MP2 CBS + Δ CCSD(T) + ZPVE	-25.10

Table 4: MP2 potential energy, enthalpy, and free energy differences between 8W, 6W, and transition state (TS). ΔH and ΔG were calculated for 298.15 K and 1 atm. Due to high computational demands, frequencies with the aug-cc-pVTZ basis set were not obtained, only Δ E for 8W and 6W systems is reported. All values are reported in kcal.mol^{-1}.

Basis set	8W - 6W	TS - 8W	TS - 6W
6-31+G*//6-31+G*	Δ E: -30.10	Δ E: 31.05	Δ E: 0.96
	Δ H: -27.14	Δ H: 25.55	Δ H: -1.59
	Δ G: -27.61	Δ G: 26.56	Δ G: -1.06
aug-cc-pVDZ//aug-cc-pVDZ	Δ E: -26.70	Δ E: 27.40	Δ E: 0.70
	Δ H: -23.30	Δ H: 21.74	Δ H: -1.56
	Δ G: -24.25	Δ G: 23.15	Δ G: -1.10
aug-cc-pVTZ//aug-cc-pVTZ	Δ E: -25.62	-	-

Table 5: DFT potential energy, enthalpy, and free energy differences between 8W, and 6W systems. ΔH and ΔG were evaluated at 298.15 K and 1 atm. All values are reported in kcal.mol^{-1}.

Level of theory	Basis set	ΔE_{8W-6W}
MP2 CBS + Δ CCSD(T)	aug-cc-pVDZ $\rightarrow$ aug-cc-pVTZ	-28.51
B3LYP	6-31+G*//6-31+G*	-25.84
	aug-cc-pVDZ//aug-cc-pVDZ	-23.06
PBE0	6-31+G*//6-31+G*	-24.24
	aug-cc-pVDZ//aug-cc-pVDZ	-22.70
BLYP	6-31+G*//6-31+G*	-22.21
	aug-cc-pVDZ//aug-cc-pVDZ	-19.25
BP86	6-31+G*//6-31+G*	-17.87
	aug-cc-pVDZ//aug-cc-pVDZ	-16.69
PBE	6-31+G*//6-31+G*	-18.81
	aug-cc-pVDZ//aug-cc-pVDZ	-17.44

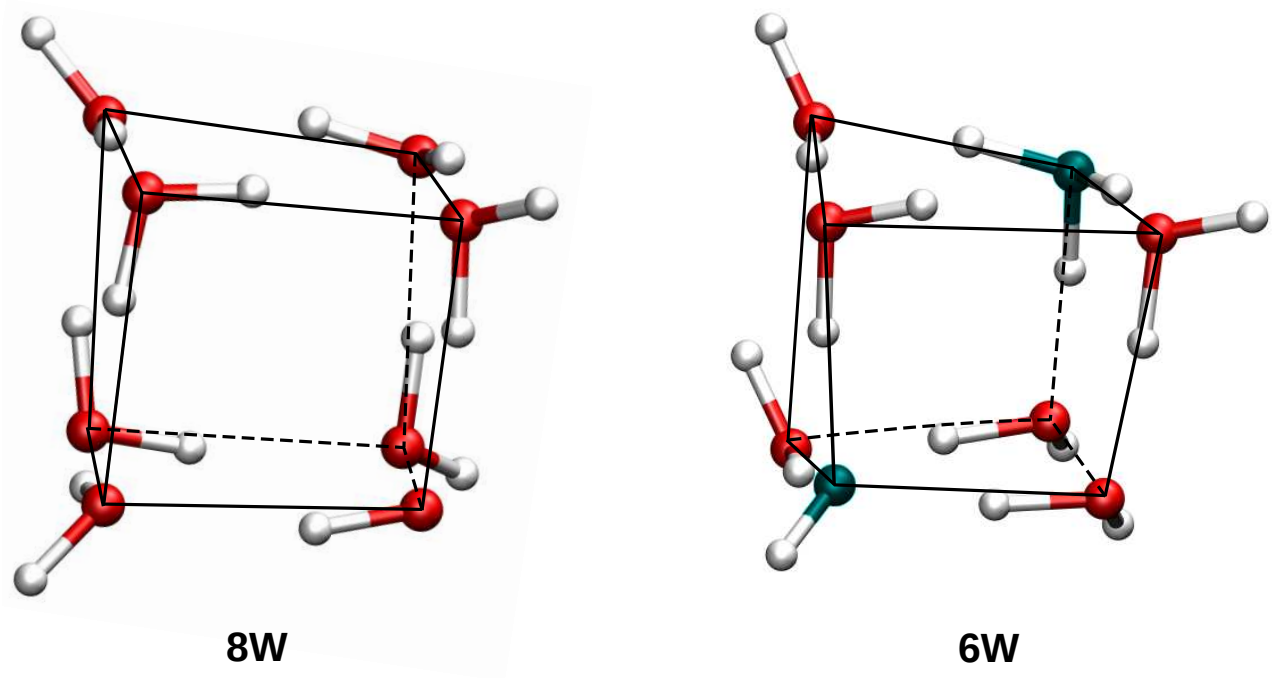

Figure 1: Structure of water octamer cluster (8W) and hydrated hydronium and hydroxide ions cluster (6W).

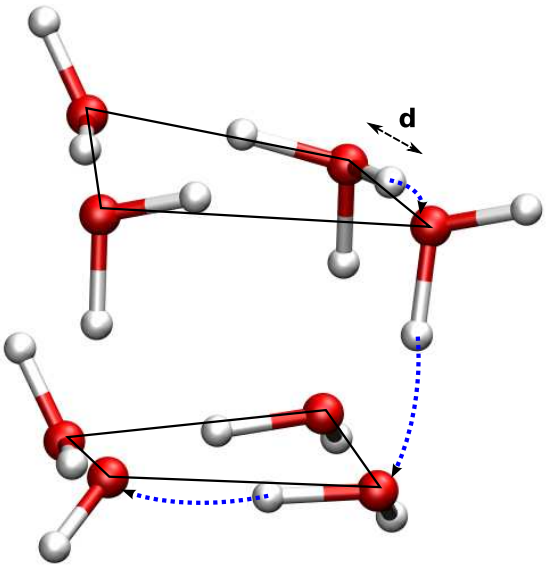

Figure 2: The change in the distance d between hydrogen and oxygen in hydronium cation (in 6W structure) triggers a proton transfer over two water molecules (displayed by blue dashed lines) resulting in the neutral water octamer 8W.

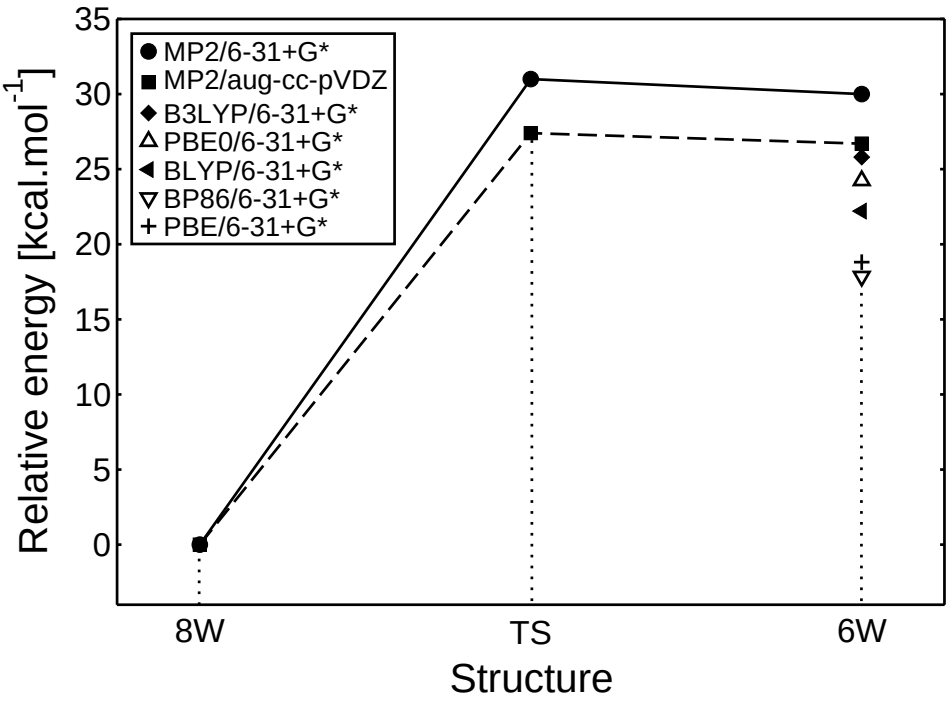

Figure 3: Relative stabilities of water octamer (8W), autoionized product (6W), and transition state between them (TS) obtained at different levels of theory. None of the density functionals was succesful in finding the transition state.